Am J Transl Res 2016;8(12):5151-5168
www.ajtr.org /ISSN:1943-8141/AJTR0011764

Original Article

Effect of early administration of lower dose versus high dose of fresh mitochondria on reducing monocrotaline-induced pulmonary artery hypertension in rat

Tien-Hung Huang[1], Sheng-Ying Chung[1], Sarah Chua[1], Han-Tan Chai[1], Jiunn-Jye Sheu[2], Yi-Ling Chen[1], Chih-Hung Chen[3], Hsueh-Wen Chang[4], Meng-Shen Tong[1], Pei-Hsun Sung[1], Cheuk-Kwan Sun[5], Hung-I Lu[2*], Hon-Kan Yip[1,6,7,8*]

[1]Division of Cardiology, Department of Internal Medicine, Kaohsiung Chang Gung Memorial Hospital and Chang Gung University College of Medicine, Kaohsiung 83301, Taiwan; [2]Division of thoracic and Cardiovascular Surgery, Department of Surgery, Kaohsiung Chang Gung Memorial Hospital and Chang Gung University College of Medicine, Kaohsiung 83301, Taiwan; [3]Divisions of General Medicine, Department of Internal Medicine, Kaohsiung Chang Gung Memorial Hospital and Chang Gung University College of Medicine, Kaohsiung 83301 Taiwan; [4]Department of Biological Sciences, National Sun Yat-Sen University, Kaohsiung 80424, Taiwan; [5]Department of Emergency Medicine, E-Da Hospital, I-Shou University School of Medicine for International Students, Kaohsiung Taiwan; [6]Center for Translational Research in Biomedical Sciences, Kaohsiung Chang Gung Memorial Hospital and Chang Gung University College of Medicine, Kaohsiung 83301, Taiwan; [7]Center for Shockwave Medicine and Tissue Engineering, Kaohsiung Chang Gung Memorial Hospital and Chang Gung University College of Medicine, Kaohsiung 83301, Taiwan; [8]Department of Medical Research, China Medical University Hospital, China Medical University, Taichung 40402, Taiwan. [*]Equal contributors.

Received June 22, 2015; Accepted July 31, 2015; Epub December 15, 2016; Published December 30, 2016

Abstract: Objective: This study aim to investigate whether early mitochondrial administration would be effective and whether high-dose mitochondria (15000 μg/rat) would be more effective than low-dose mitochondria (1500 μg/rat) for attenuating the monocrotaline (MCT/65 mg/kg/rat)-induced pulmonary artery hypertension (PAH) in rat. Method and results: Male-adult SD rats (n = 32) were randomized categorized into groups 1 (sham-control), 2 (PAH), 3 (PAH + low-dose mitochondria), and 4 (PAH + high-dose mitochondria). Mitochondria were admitted at day 5 and rats were sacrificed at day 35 post-MCT treatment. By day 35, oxygen saturation (saO_2) was highest in group 1 and lowest in group 2, and significantly higher in group 3 than in group 4 (P<0.001). Conversely, right ventricular systolic blood pressure showed an opposite pattern compared with saO_2 among all groups (P<0.001). Histological integrity of alveolar sacs exhibited a pattern identical to saO_2, whereas lung crowding score and number of muscularized artery displayed an opposite pattern (all P<0.001). The protein expression of indices of inflammation (MMP-9, TNF-α, NF-κB), oxidative stress (oxidized protein, NO-1, NOX-2, NOX-4), apoptosis (Bax, cleaved caspase-3 and PARP), fibrosis (p-Smad3, TGF-β), mitochondrial-damage (cytosolic cytochrome-C), and hypoxia-smooth muscle proliferative factors (HIF-α, connexin43, TRPCs) showed an opposite pattern compared, whereas anti-fibrosis (p-Smad1/5, BMP-2) and mitochondrial integrity (mitochondrial cytochrome-C) exhibited an identical pattern to saO_2 in all groups (all P<0.001). Conclusion: Low dose is superior to high dose of mitochondria for protecting against MCT-induced PAH. The paradoxical beneficial effect may imply therapy with 15000 μg/rat mitochondria is overdose in this situation.

Keywords: Mitochondria, pulmonary arterial hypertension, oxidative stress, smooth muscle proliferation

Introduction

Pulmonary arterial hypertension (PAH) exhibits a particular subset of pulmonary hypertension fitting within Group 1 of the World Health Organization (WHO) classification system [1]. Hemodynamic and histopathological findings of PAH which have been keenly investigated is characterized by abnormal elevation in mean pulmonary artery pressure and pulmonary vascular resistance and progressively increased in remodeling of the pulmonary vasculature char-

acterized by proliferation of smooth muscle cells with intimal fibrosis, medial hypertrophy, and adventitial thickening [2-7] which, in turn, causes right-side heart failure [1, 2, 8] with a progressive course and poor prognosis. The life expectancy of patients suffering from the disease is extremely short without treatment (i.e. an average of 2.8 years from diagnosis) [2, 4, 5, 7].

Although the pathogenesis of PAH is multifactorial, progressive endothelial cell dysfunction seems to play a crucial role for PAH [9-12]. Additionally, oxidative stress has been identified as an essential role to contribute the development and progression of PAH as well as aggravate the progressive course of PAH [13]. Intriguingly, one recent study has shown that S-nitroso human serum albumin reduces pulmonary hypertension and improves right ventricular (RV) systolic and diastolic function and RV-arterial coupling, with a positive effect on ventricular interdependence by increasing energetic reserve and reducing oxidative stress [14]. Basic on the results of these studies [13, 14], the strategic management of early energetic reserve and reducing oxidative stress which would inhibit endothelial dysfunction and death, followed by preventing smooth muscle proliferation may be a new therapeutic option for PAH.

Despite mitochondria are the major energy source for supplying the cellular requirement for metabolisms, activity and survive, mitochondria are an additional major source for the generation of reactive oxygen species (ROS) and recent data suggest that ROS produced by NADPH oxidase may contribute to the alteration in mitochondrial function [15]. On the other hand, exogenous mitochondrial transfusion has recently been shown to effectively protect against acute organ damage, including sepsis-induced acute lung injury [16] and acute ischemia-reperfusion injury of the heart [17] and liver [18] manily through refreshing the endogeneous mitochondria in the injuried cells/organs. Thus, “mitochondria” is the “double edged sword”, depending on how to utilize this energetic reserve. Intriguingly, our more recent study has shown that mitochondrial treatment effectively protected the lungs against 100% oxygen inhalation-induced acute respiratory distress syndrome (ARDS) at molecular, cellular, structural, and functional levels in a rodent model. However, whether such a therapeutic modality for PAH has not been reported currently. Accordingly, by utilizing a monocrotaline (MCT)-induced PAH rodent animal model, this study tested the hypothesis that (1) mitochondrial transfusion might offer a beneficial effect on attenuating MCT-induced PAH, and (2) high dose of mitochondria (15000 ug/rat) would be superior to low dose of mitochondria for protecting against MCT-induced PAH.

Materials and methods

Ethics

All animal experimental procedures were approved by the Institute of Animal Care and Use Committee at Kaohsiung Chang Gung Memorial Hospital (Affidavit of Approval of Animal Use Protocol No. 2014071601) and performed in accordance with the Guide for the Care and Use of Laboratory Animals (NIH publication No. 85-23, National Academy Press, Washington, DC, USA, revised 1996).

Animal models of PAH

On day 0, 32 pathogen-free, adult male Sprague-Dawley (SD) rats, weighing 350-365 g (Charles River Technology, BioLASCO Co., Ltd., Taiwan), were given one subcutaneous injection of MCT (65 mg/kg; Sigma, St. Louis, MO). These MCT-treated animals were then assigned to three groups: group 2 (MCT alone, n = 8), group 3 [MCT + low dose of mitochondria (1500 μg/rat), n = 8)], and group 4 [MCT + high dose of mitochondria (15000 μg/rat), n = 8]. Another group of eight SD rats (group 1, n = 8) receiving only subcutaneous injection of 3 mL normal saline served as sham controls. The dosage of MCT (65 mg/kg) was based on our previous studies [10, 19].

Intravenously mitochondrial transfusion to animals in groups 3 and 4 was performed on day 5 after MCT injection based on our previous study [10] that demonstrated the effectiveness of early treatment in reducing MCT-induced rat PAH.

Mitochondrial isolation and mitotracker staining for mitochondria

The procedure and protocol for mitochondrial isolation and mitotracker staining has been described in our recent report [20]. Liver mito-

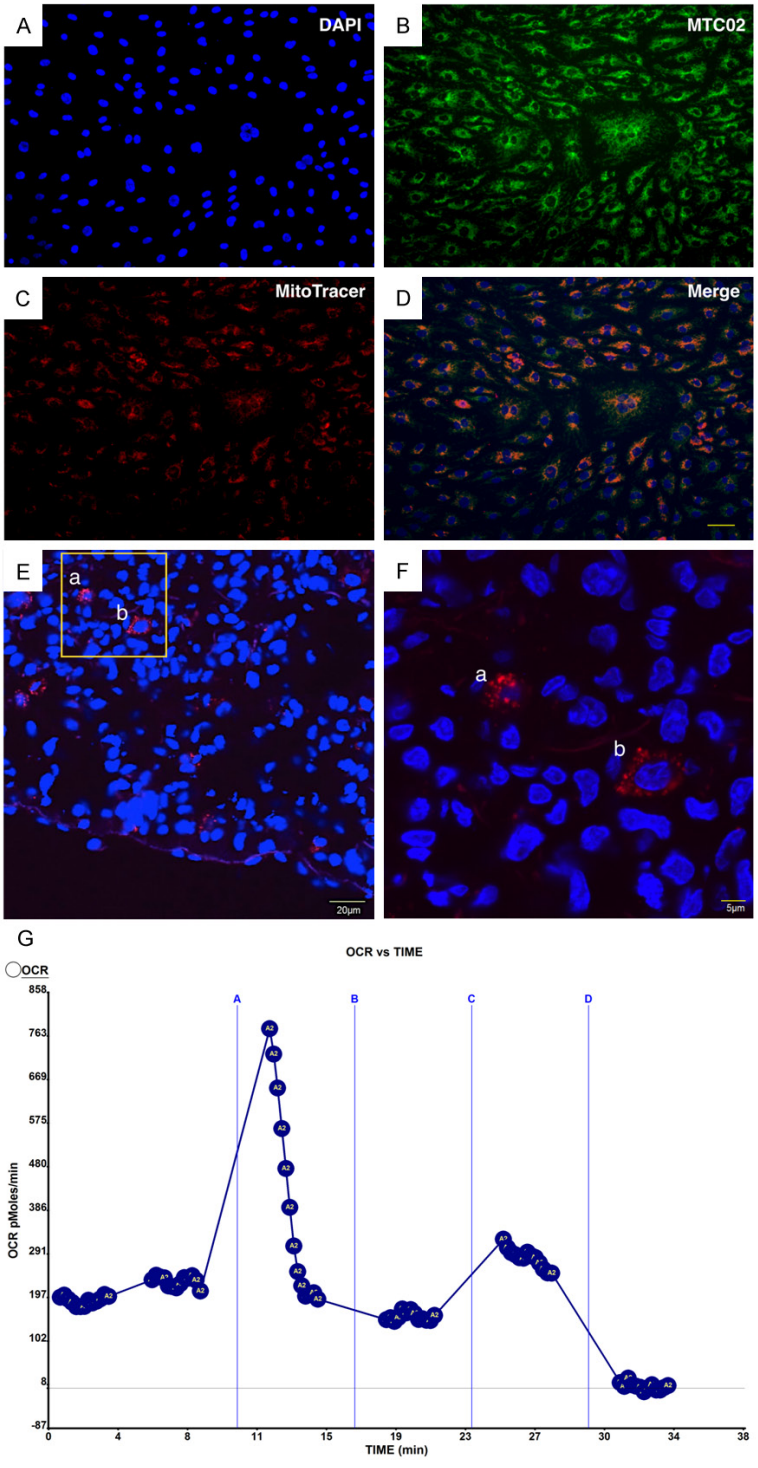

Figure 1. Evidences of successful mitochondrial transfusion into the cells and high oxygen consumption rate of isolated mitochondria. (A) DAPI stain (200×) for identification of nuclei of in human umbilical vein endothelial cells (HUVECs). (B) Immunofluorescent (IF) microscopic finding (200×) showing the expression of the total mitochondria (green color) (i.e., exogenous and endogenous) in HUVECs. (C) IF microscopic finding (200×) (MitoTracer dye stained mitochondria) illustrating the successful transfusion of exogenous mitochondria (red color) in human umbilical vein endothelial cells (HUVECs). (D) IF microscopic finding (200×) illustrating the merged (C & D) pictures, indicating the presence of exogenous and endogenous mitochondria in HUVECs. The scale bars in right lower corner represent 50 μm. (E) Confocal microscopic finding showing numerous exogenous mitochondria (red color) had been successfully transfused into the lung parenchyma. (F) Illustrating the magnified (a) and (b) in small square in (E to F). The a and b in (F) indicated the exogenous mitochondria were successfully transfused into the lung parenchyma. (G) Illustrating the high oxygen consumption rate of isolated mitochondria for ready to be utilized.

chondria were isolated from donor rats. In details, the rats were starved overnight prior to mitochondrial isolation. The rats were sacrificed and the gallbladder and liver were removed. Immediately, the liver (3 g) were immersed in 50 mL of ice-cold IBc (10 mM Tris-MOPS, 5 mM EGTA/Tris and 200 mM sucrose, pH 7.4.) in a small beaker, followed by rinsing the liver free of blood by using ice-cold IBc. The liver was then minced into small pieces using scissors in a beaker surrounded by ice. IBc were discarded during the mincing and replaced with 18 mL of ice-cold fresh IBc. The liver was then homogenized using a Teflon pestle. The homogenate were transferred to a 50 mL polypropylene Falcon tube and then centrifuged at 600 g for 10 minutes at 4°C. The supernatants were again transferred to centrifuge tubes for centrifugation at 7,000 g for 10 minutes at 4°C. The supernatants were discarded and the pellets were washed with 5 mL ice-cold IBc. Again, the supernatants from pellets were centrifuged at 7,000 g for 10 minutes at 4°C. The supernatants were discarded the pellets which contained the mito-

chondria were resuspended again. The concentration of the mitochondrial suspensions was measured using the Biuret method. Each 10 mg of isolated mitochondria were labeled with 1 M of MitoTracker Red CMXRos (Invitrogen, Carlsbad, CA) through incubation at 37°C for 30 minutes. Intravenously mitochondrial transfusion was performed for the study animals in groups 3 and 4 immediately after labeling (i.e., <3 hrs after the isolation procedure, **Figure 1**).

Procedure and protocol for quantification of oxygen consumption rate (OCR) of isolated mitochondria (Seahorse method)

The procedure and protocol for quantification of ROC of isolated mitochondria was based on our recent report [20], In details, functional activity of isolated mitochondria from rat liver was determined by an Extracellular Flux Analyzer (XF^e24, Seahorse Bioscience, MA, USA) through assessing the degree of coupling between the electron transport chain (ETC) and the oxidative phosphorylation machinery (OXPHOS). Bioenergetics of mitochondria as reflected in the integrity of electron transport chain and capacity of oxidative phosphorylation were evaluated by measuring the OCR. In the present study, isolated mitochondria (10 μg/well) from rat liver were diluted in cold 1× mitochondria assay solution (MAS) (70 mM sucrose, 220 mM mannitol, 10 mM KHPO, 5 mM $MgCl_2$, 2 mM HEPES, 1.0 mM EGTA and pH 7.2), followed by spinning down at 3000 g for 30 minutes. After attachment of mitochondria to XF24 plate, coupling reaction was initiated with the administration of substrate (10.0 mM succinate). State 3 was initiated with ADP (0.5 mM), while state 4 was induced with the addition of oligomycin (2 μM). Maximal uncoupler-stimulated respiration was elicited with FCCP (4 μM), whereas complex III repression was induced by antimycin A (4 μM). OCR of mitochondria in reactions mentioned above was sequentially measured (**Figure 1G**).

Determination of arterial oxygen saturation (saO_2), hemodynamic assessment and specimen preparation

To investigate the therapeutic effect of mitochondria treatment on saO_2, arterial blood was sampled from the carotid artery for blood gas analysis prior to intubation and ventilator use.

The protocol and procedure of hemodynamic measurement were previously described [10, 19, 20]. On day 90 after MCT treatment, the rats were anesthetized by inhalation of 2.0% isoflurane. Blood (1.0 mL) was sampled from the tail artery for measuring arterial oxygen saturation. After being shaved on the chest, each animal was endotracheally intubated with positive-pressure ventilation (180 mL/min) with room air using a small animal ventilator (SAR-830/A, CWE Inc., U.S.A.). The heart was exposed by left thoracotomy. A sterile 20-gauge, soft-plastic coated needle was inserted into the right ventricle and femoral artery of each rat to measure the right ventricular systolic blood pressure (RVSBP) and arterial systolic blood pressure, respectively, when heart rate >310 beat/min. The pressure signals were first transmitted to a pressure transducer (UFI, model 1050, CA, U. S. A.) and then exported to a bridge amplifier (ML866 Power Lab 4/30 Data Acquisition Systems. AD Instruments Pty Ltd., Castle Hill, NSW, Australia) where the signals were amplified and digitally recorded. The data were recorded and later analyzed with the Lab chart software (AD Instrument). After hemodynamic measurements, the rats were euthanized with the hearts and lungs harvested. For each animal, the interventricular + left ventricular weight and right ventricular weigh were recorded from which the ratio of right ventricle to interventricular septal plus left ventricular weight was calculated.

The preparation of lung specimens for morphometric analyses were based on our recent reports [10, 19, 20]. Briefly, the left lung were inflated at a constant airway pressure (15-20 mmHg) and fixed with OCT (Tissue-Tek) for immunohistochemical staining. The right lung was then cut into pieces that were either fixed in 4% paraformaldehyde/0.1% glutaradehyde PBS solution before being embedded in paraffin blocks for hematoxylin-eosin staining or stored at -80°C for protein and mRNA analyses.

Histological assessment of lung injury

The lung specimens were sectioned at 5 μm for light microscopy. H&E staining was performed to estimate the number of alveolar sacs in a blinded fashion as we previously reported [10, 19-21]. Three lung sections from each rat were analyzed and three randomly selected high-power fields (HPFs; 100×) were examined in each section. The mean number per HPF for each animal was then determined by summation of all numbers divided by 9. The extent of

crowded area, which was defined as region of thickened septa in lung parenchyma associated with partial or complete collapse of alveoli on H&E-stained sections, was also performed in a blinded fashion. The following scoring system [15] was adopted: 0 = no detectable crowded area; 1≤15% of crowded area; 2 = 15-25% of crowded area; 3 = 25-50% of crowded area; 4 = 50-75% of crowded area; 5≥75%-100% of crowded area/HPF.

Histological quantification of lung fibrotic tissue

The procedure and protocol were described in our previous report [22]. Masson's trichrome staining was used to identify fibrosis of the lung parenchyma. Three serial sections of lung tissue in each animal were prepared at 4 μm thickness by Cryostat (Leica CM3050S). The integrated area (μm^2) of fibrosis on each section were calculated using Image Tool 3 (IT3) image analysis software (University of Texas, Health Science Center, San Antonio, UTHSCSA; Image Tool for Windows, Version 3.0, USA). Three randomly selected high-power fields (HPFs) (100×) were analyzed in each section. After determining the number of pixels in each infarct and fibrotic area per HPF, the numbers of pixels obtained from three HPFs were summated. The procedure was repeated in two other sections for each animal. The mean pixel number per HPF for each animal was then determined by summating all pixel numbers and dividing by 9. The mean integrated area (μm^2) of fibrosis in lung per HPF was obtained using a conversion factor of 19.24 (1 μm^2 represented 19.24 pixels).

Western blot analysis of lung tissue

Equal amounts (50 mg) of protein extracts were loaded and separated by SDS-PAGE using acrylamide gradients. After electrophoresis, the separated proteins were transferred electrophoretically to a polyvinylidene difluoride (PVDF) membrane (Amersham Biosciences). Nonspecific sites were blocked by incubation of the membrane in blocking buffer [5% nonfat dry milk in T-TBS (TBS containing 0.05% Tween 20)] overnight. The membranes were incubated with the indicated primary antibodies [matrix metalloproteinase (MMP)-9 (1:1000, Millipore), tumor necrosis factor (TNF)-α (1:1000, Cell Signaling), nuclear factor (NF)-κB (1:1000, Abcam), NOX-1 (1:1500, Sigma), NOX-2 (1: 750, Sigma), NOX-4 (1:1000, Abcam), Bax (1: 1000, Abcam), caspase 3 (1:1000, Cell Signaling), poly (ADP-ribose) polymerase (PARP) (1:1000, Cell Signaling), phosphorylated (p)-Smad3 (1:1000, Cell Signaling), p-Smad1 (1:500, Abcam), p-smad5 (1:1000, Abcam), bone morphogenic protein (BMP) 2 (1:5000, Abcam) transforming growth factor (TGF)-β (1:500, Abcam), connexin(Cx)43 (1:2000, Millipore), hypoxia-inducible factor (HIF)-1α (1:750, Abcam), transient receptor potential cation channel 1 (TRPC1) (1:1000, Abcam), TRPC4 (1:600, Abcam), TRPC6 (1:1000, Abcam), cytosolic cytochrome C (1:2000, BD), mitochondria cytochrome C (1:2000, BD) and Actin (1: 10000, Chemicon)] for 1 hour at room temperature. Horseradish peroxidase-conjugated anti-rabbit immunoglobulin IgG (1:2000, Cell Signaling) was used as a secondary antibody for one hour at room temperature. The washing procedure was repeated eight times within one hour, and immunoreactive bands were visualized by enhanced chemiluminescence (ECL; Amersham Biosciences) and exposed to Biomax L film (Kodak). For purposes of quantification, ECL signals were digitized using Labwork software (UVP).

Distribution of alveolar sacs, crowded score, and arterial muscularization in lung parenchyma

Left lung specimens from all animals were fixed in 10% buffered formalin before being embedded in paraffin and sectioned at 5 μm for light microscopic analysis. Hematoxylin and eosin (H&E) staining was performed to determine the number of alveolar sacs according to our recent study [10, 19-21] in a blind fashion. Three lung sections from each rat were analyzed and three randomly selected HPFs (100×) were examined in each section. The number of alveolar sacs was recorded for each animal. The mean number per HPF for each animal was then determined by summation of all numbers divided by 9.

The percentage of crowded area (defined as septal thickness associated with partial or complete collapse of alveoli) in lung parenchyma was determined using H&E staining in a blind fashion and scored as follows: 0 = no detectable crowded area; 1≤15% of crowded area; 2 = 15-25% of crowded area; 3 = 25-50%

of crowded area; 4 = 50-75% of crowded area; 5≥75%-100% of crowded area/per high-power field (100×)]. The procedure and protocol were based on our previous reports [10, 19-21].

The detailed procedure and protocol for determining muscularization (i.e., an index of vascular remodeling) of pulmonary arterioles was described in details in our previous report [19]. Briefly, three measurements were taken for the thickness of pulmonary arterioles. Muscularization of the arterial medial layer in lung parenchyma was defined as a mean thickness of vessel wall greater than 50% of the lumen diameter in a vessel of diameter >30 μm. Measurement of arteriolar diameter and wall thickness was achieved using the Image-J software (NIH, Maryland, USA).

Oxidative stress measurement of lung parenchyma

The procedure and protocol for assessing the protein expression of oxidative stress have been detailed in our previous reports [22, 23]. The Oxyblot Oxidized Protein Detection Kit was purchased from Chemicon (S7150). DNPH derivatization was carried out on 6 μg of protein for 15 minutes according to the manufacturer's instructions. One-dimensional electrophoresis was carried out on 12% SDS/polyacrylamide gel after DNPH derivatization. Proteins were transferred to nitrocellulose membranes which were then incubated in the primary antibody solution (anti-DNP 1:150) for 2 hours, followed by incubation in secondary antibody solution (1:300) for 1 hour at room temperature. The washing procedure was repeated eight times within 40 minutes. Immunoreactive bands were visualized by enhanced chemiluminescence (ECL; Amersham Biosciences) which was then exposed to Biomax L film (Kodak). For quantification, ECL signals were digitized using Labwork software (UVP). For oxyblot protein analysis, a standard control was loaded on each gel.

Immunofluorescent (IF) staining

IF staining was performed using respective primary antibodies for the examinations of γ-H2AX+ (1:500, Abcam), TRPC1+ (1:100, Abcam), TRPC4+ (1:200, Abcam), TRPC6+ (1:200, Abcam) and HIF-1α+ (1:100, Abcam; 1:300, Novus) cells and Actinin-phalloidin (1:500, LuBio Science; 1:500, Life Technologies) in lung based on our previous studies [10, 19-21]. Irrelevant antibodies were used as controls in the current study.

Distribution of small vessels in lung parenchyma

The detailed procedure and protocol have been described in our recent reports [10, 12]. Briefly, IHC staining of α-smooth muscle actin using the appropriate antibodies (Sigma) was performed to identify pulmonary arterioles according to manufacturer's instructions. Three lung sections from each rat were analyzed and three randomly selected HPFs (100×) were analyzed in each section. The mean number per HPF for each animal was then determined by summation of all numbers divided by 9.

Statistical analyses

Quantitative data are expressed as mean ± SD. Statistical analysis was performed by ANOVA followed by Bonferroni multiple-comparison *post hoc* test. All analyses were conducted using SAS statistical software for Windows version 8.2 (SAS institute, Cary, NC). A probability value <0.05 was considered statistically significant.

Results

In vitro and in vivo studies proved the successful mitochondrial transfusion into the cells and isolated mitochondria with high activity

To determine whether mitochondria was successfully transfused into the cells after exposure to hypoxia, HUVECs (5.0×10^6 cells) were cultured in hypoxia chamber (1.5% of oxygen) for six hours prior being collected for mitochondrial transfusion (750 μg). Examination of the cells with IF imaging showed copious mitochondria in the HUVECs (**Figure 1A-D**).

To elucidate whether mitochondria was successfully transfused in the lung parenchyma, additional four rats received low-dose mitochondria (1500 μg/rat, n = 2) and high-dose mitochondria (15000 μg/rat, n = 2) by day 5 after MCT treatment. The animals were sacrificed 3 h later after mitochondrial transfusion and the lung tissues were well prepared for IF image study. The results showed that abundant exogenous mitochondria were found in the lung parenchyma (**Figure 1E** and **1F**).

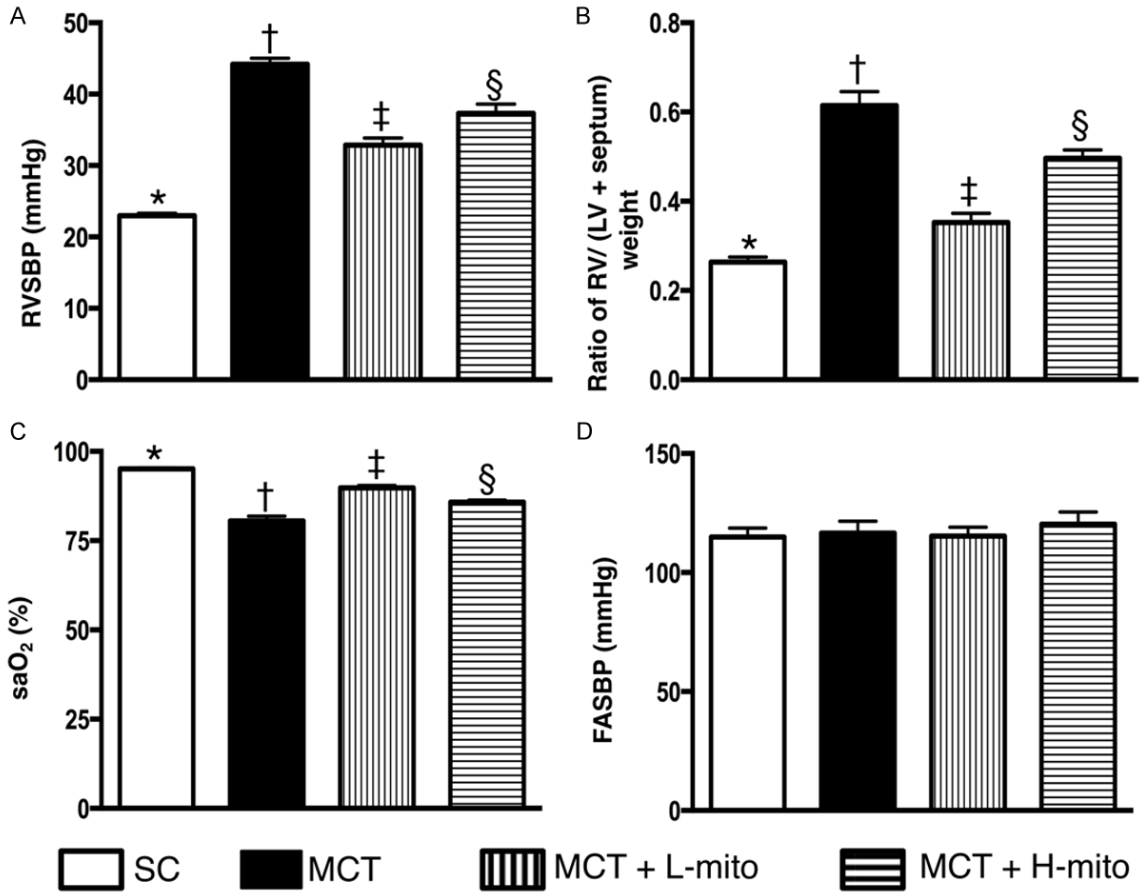

Figure 2. Arterial oxygen saturation, RVSBP, and ratio of RV weight to LV+ septal weight by day 35 after MCT administration. A. Right ventricular systolic blood pressure (RVSBP), * vs. other groups with different symbols (*, †, ‡, §), P<0.0001. B. The ratio of right ventricular (RV) weight to septum + left ventricular (LV) weight, * vs. other groups with different symbols (*, †, ‡, §), P<0.001. C. Arterial oxygen saturation (%), * vs. other groups with different symbols (*, †, ‡, §), P<0.001. D. The femoral arterial systolic blood pressure (FASBP), control vs. other groups, p>0.5. All statistical analyses were performed by one-way ANOVA, followed by Bonferroni multiple comparison post hoc test. Symbols (*, †, ‡, §) indicate significance (at 0.05 level). SC = sham control; MCT = monocrotaline; L-mito = low dose of mitochondria; H-mito = high dose of mitochondria.

To assess the function of isolated mitochondria, the OCR was determined by the Mito stress test kit (i.e., Seahorse Bioscience, Billerica, MA) and the XF24 Analyzer. The results (i.e., OCR, **Figure 1G**) illustrated very satisfactory mitochondrial activity for the purpose of the present study.

Arterial oxygen saturation, hemodynamics, and ratio of RV weight to LV+ septal weight by day 35 after MCT administration

By day 35 after MCT administration, the RVSBP, an index of systolic pulmonary artery blood pressure, was highest in group 2 (MCT only) and lowest in group 1 (SC), and significantly higher in group 4 (MCT + high dose of mitochondria) than in group 3 (MCT + low dose of mitochondria). Additionally, the ratio of RV weight to septum + left ventricular weight, exhibited an identical pattern of RVSBP among the four groups. On the other hand, the percentage of saO_2 showed an opposite pattern of RVSB among the four groups (**Figure 2**). However, the femoral arterial blood pressure did not differ among the four groups.

Histopathological findings of lung parenchyma by day 35 after MCT administration

The number of alveolar sacs was highest in group 1 and lowest in group 2, and significantly higher in group 3 than in group 4 (**Figure 3**). Conversely, the lung parenchyma was most

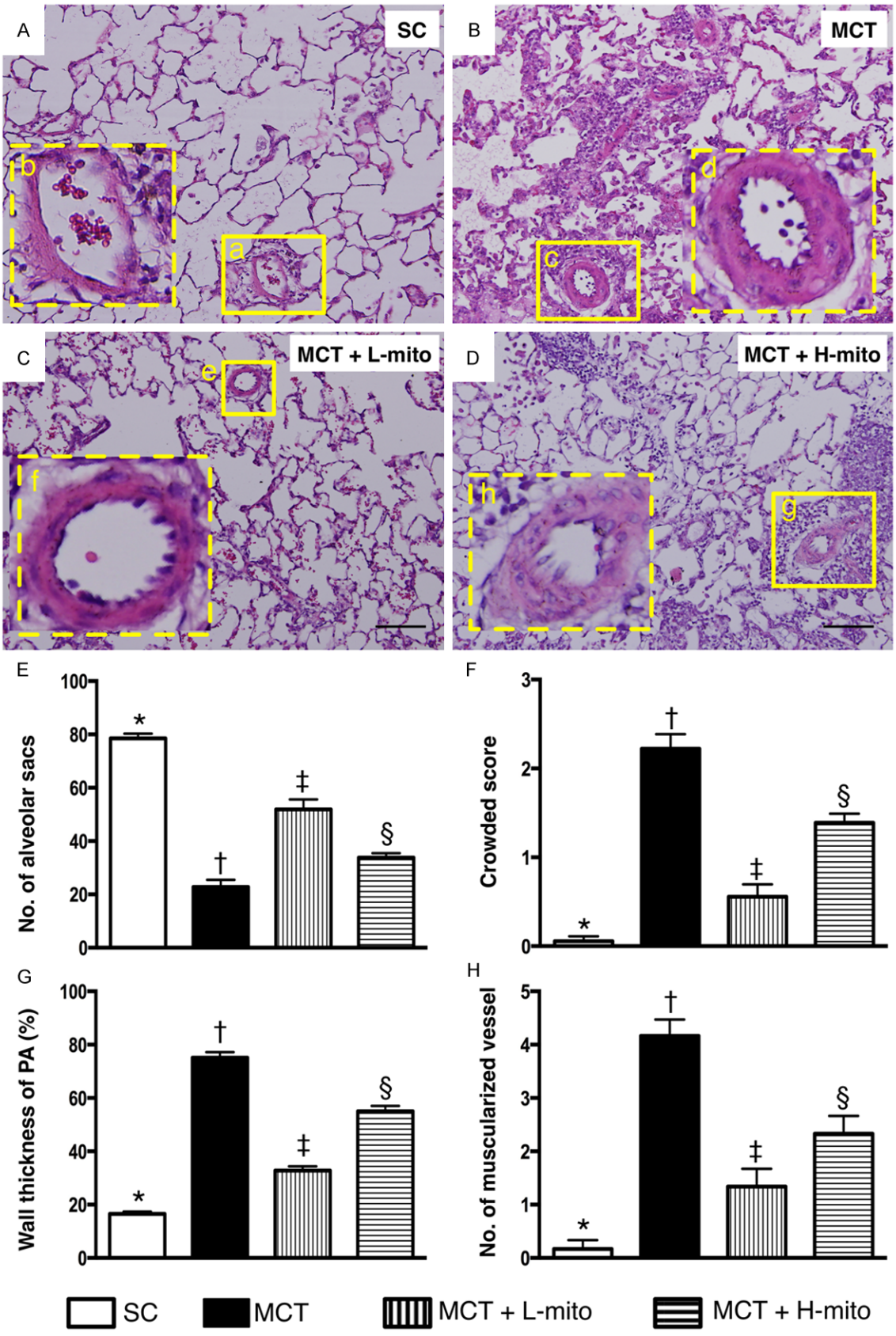
A
SC
B
MCT
C
MCT + L-mito
D
MCT + H-mito
a
b
c
d
e
f
g
h
E
No. of alveolar sacs
F
Crowded score
G
Wall thickness of PA (%)
H
No. of muscularized vessel
SC
MCT
MCT + L-mito
MCT + H-mito

Figure 3. Histopathological findings of lung parenchyma by day 35 after MCT administration. A-D. Microscopic finding (100×) of H&E stain of lung parenchyma. Solid-line small squares (a, c, e, g) were magnified into dotted-line large squares (b, d, f, h) for the purpose of more clear identification of thickness of smooth muscle layer of pulmonary artery (PA). The results showed typical muscularization of PA in the lung parenchyma. E. Analytic result of number of alveolar sacs, * vs. other groups with different symbols (*, †, ‡, §), P<0.0001. F. Analytic result of crowded score of lung parenchyma, * vs. other groups with different symbols (*, †, ‡, §), P<0.0001. G. Analytical result of wall thickness of PA, * vs. other groups with different symbols (*, †, ‡, §), P<0.0001. H. Analytical result of number of muscularized PAs, * vs. other groups with different symbols (*, †, ‡, §), P<0.001. The scale bars in right lower corner represent 100 μm. All statistical analyses were performed by one-way ANOVA, followed by Bonferroni multiple comparison post hoc test. Symbols (*, †, ‡, §) indicate significance (at 0.05 level). SC = sham control; MCT = monocrotaline; L-mito = low dose of mitochondria; H-mito = high dose of mitochondria.

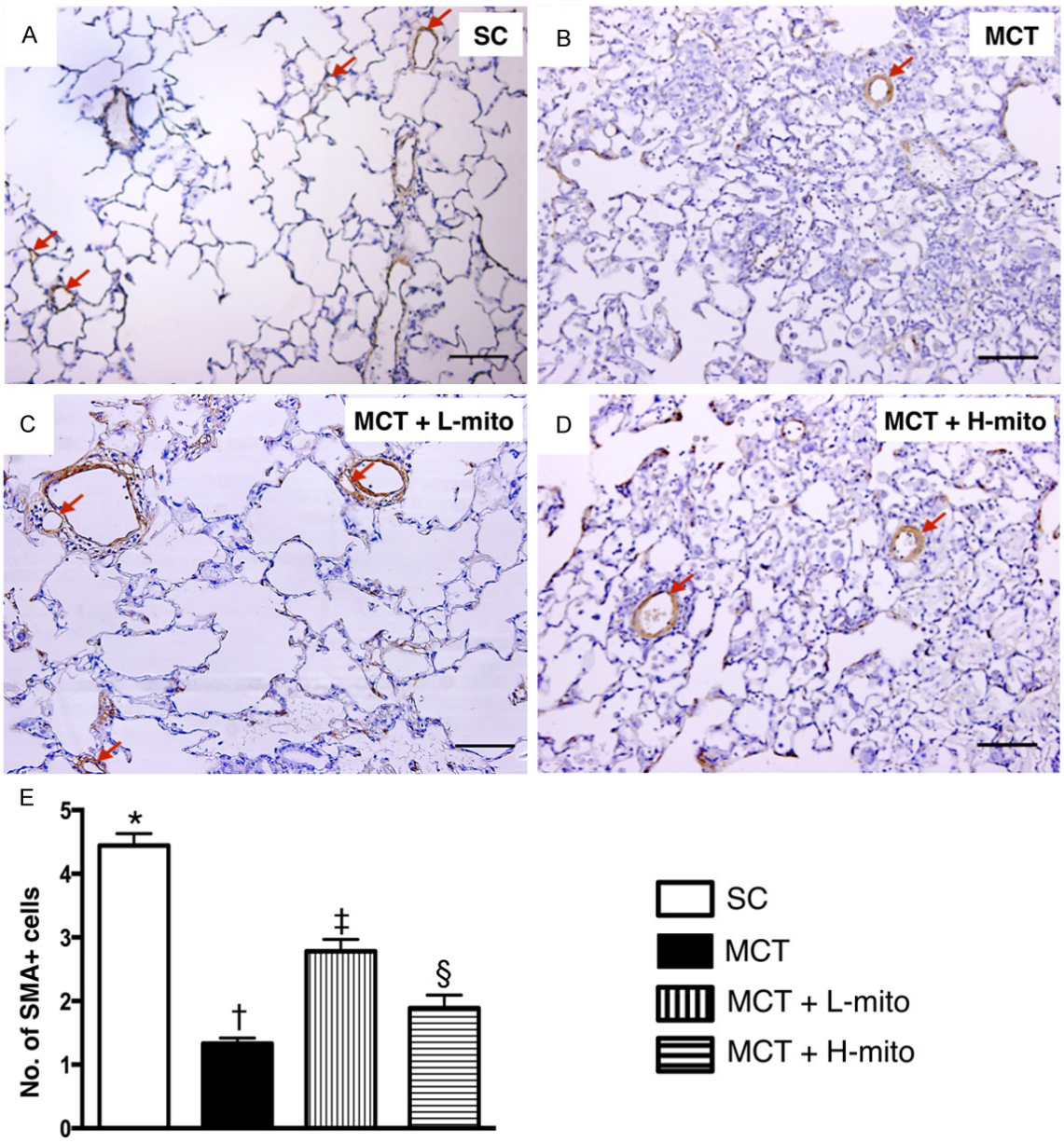

Figure 4. Numbers of small vessels in lung parenchyma by day 35 after MCT administration. A-D. Microscopic finding (100×) of immunohistochemical staining [(i.e., α-smooth muscle actin stain (α-SMA)]w for identifying the number of small pulmonary arterioles (PAs) in lung parenchyma (red arrows). E. Analytical result of number of small PAs, * vs. other groups with different symbols (*, †, ‡, §), P<0.001. The scale bars in right lower corner represent 100 μm. All statistical analyses were performed by one-way ANOVA, followed by Bonferroni multiple comparison post hoc test. Symbols (*, †, ‡, §) indicate significance (at 0.05 level). HPF = high-power field; SC = sham control; MCT = monocrotaline; L-mito = low dose of mitochondria; H-mito = high dose of mitochondria.

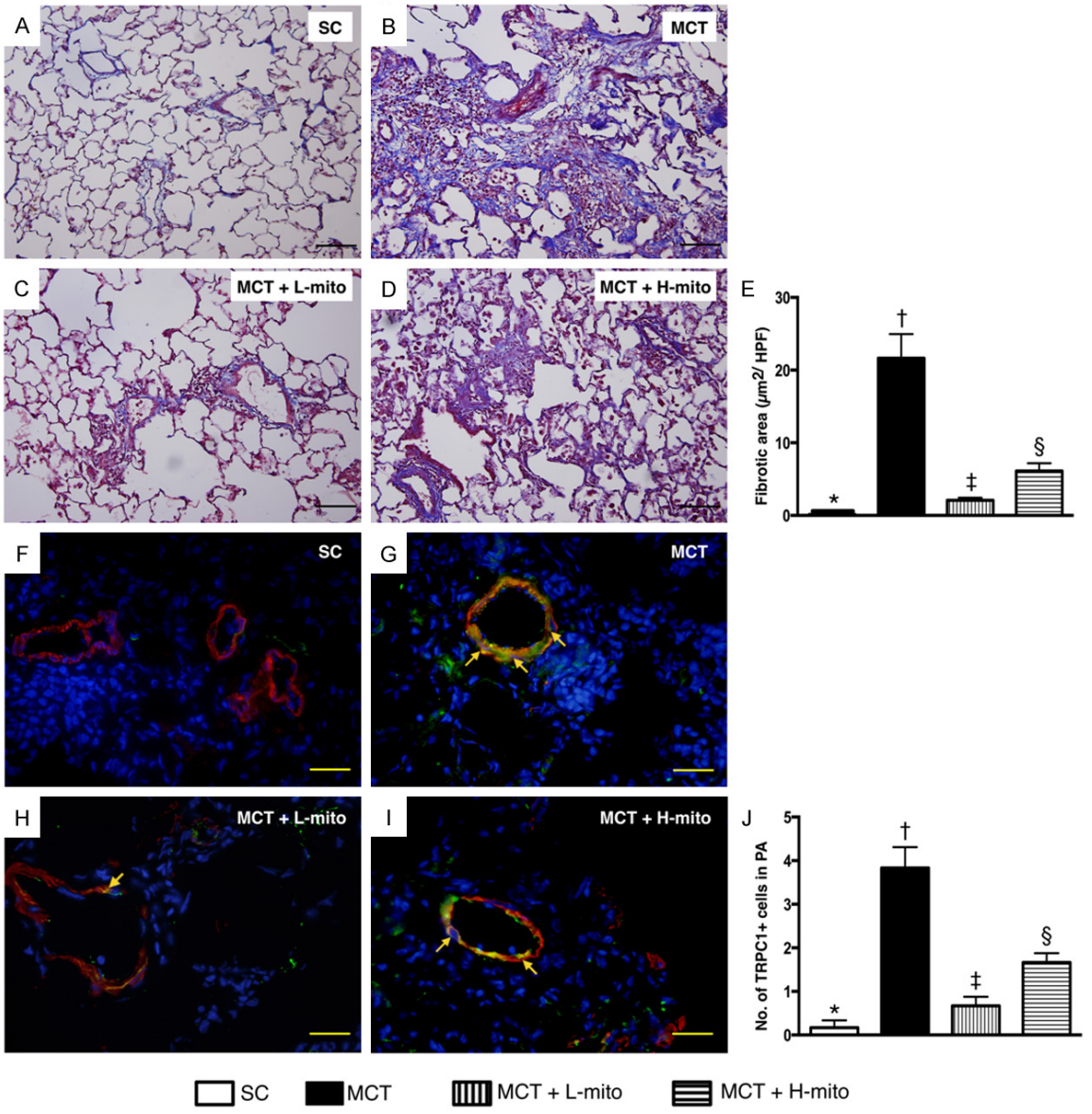

Figure 5. The fibrosis in lung parenchyma and expressions of transient receptor potential cation channel (TRPC1) in pulmonary artery by day 35 after MCT administration. A-D. Immunohistochemical staining (i.e., Mason's trichrome stain) (100×) for identification of fibrotic area in lung parenchyma. E. Analytical result of fibrotic area, * vs. other groups with different symbols (*, †, ‡, §), P<0.0001. The scale bars in right lower corner represent 100 μm. F-I. Immunofluorescent microscopic finding (400×) for identification of TRPC1+ cells (yellow arrows) in pulmonary artery (PA). J. Number of TRPC1+ cells, * vs. other groups with different symbols (*, †, ‡, §), P<0.001. The scale bars in right lower corner represent 20 μm. All statistical analyses were performed by one-way ANOVA, followed by Bonferroni multiple comparison post hoc test. Symbols (*, †, ‡, §) indicate significance (at 0.05 level). SC = sham control; MCT = monocrotaline; L-mito = low dose of mitochondria; H-mito = high dose of mitochondria.

crowded in group 2, significantly crowed in groups 3 and 4 than that in group 1, and significantly crowed in group 4 than that in group 3 (**Figure 3**).

The histopathological analysis using H&E staining revealed that the wall thickness of pulmonary arterioles and number of muscularized arterioles (**Figure 3**) exhibited an identical pattern compared to that of the crowded score among the four groups. On the other hand, IHC staining for α-smooth muscle actin demonstrated that the number of small arterioles in lung parenchyma showed an identical pattern of number of alveolar sacs among the four groups (**Figure 4**).

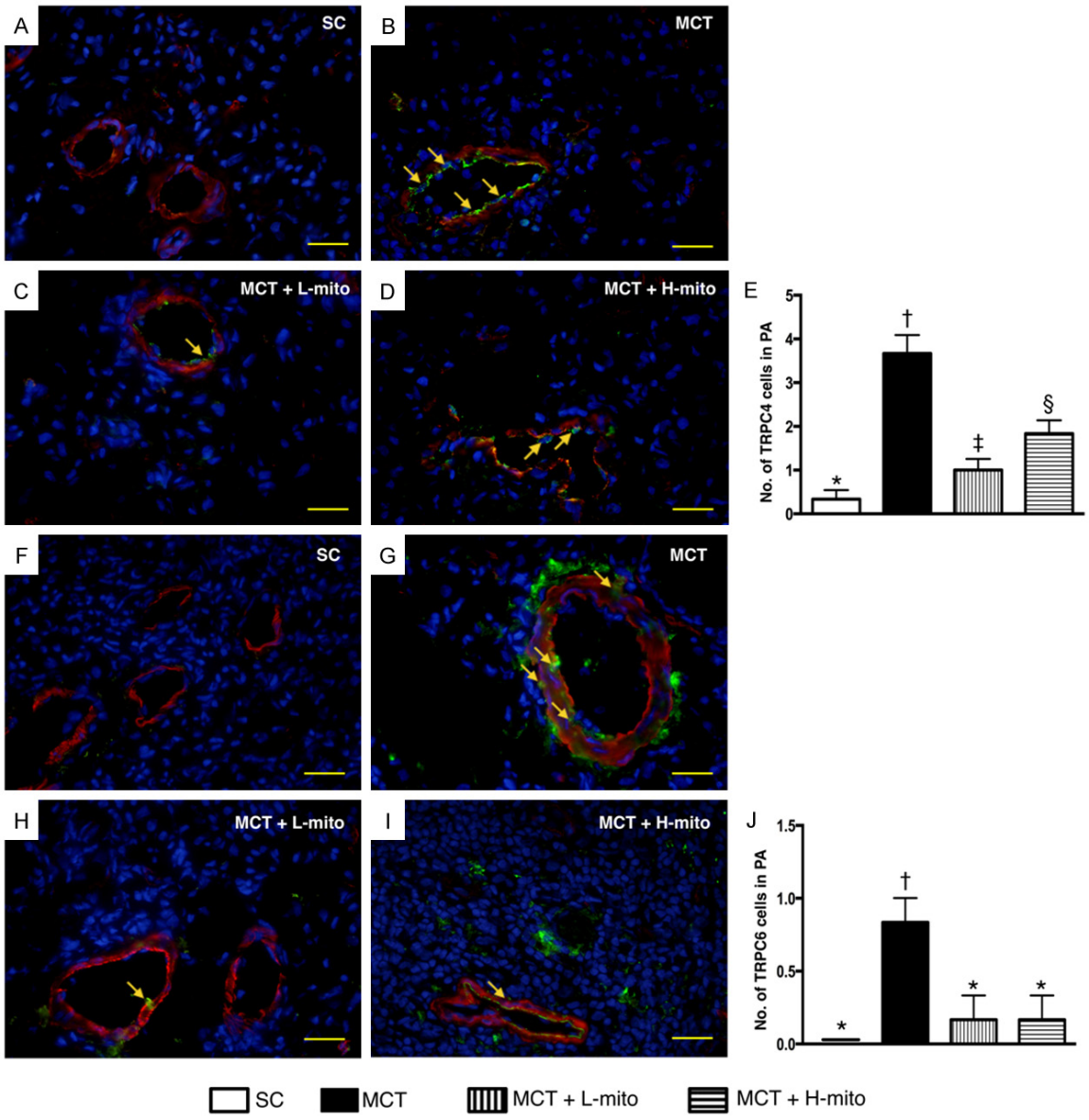

Figure 6. Expressions of transient receptor potential cation channels 4 & 6 (TRPCs4 and 6) in pulmonary artery by day 35 after MCT administration. A-D. Immunofluorescent (IF) microscopic finding (400×) for identification of TRPC4+ cells (yellow arrows) in pulmonary artery (PA). E. Number of TRPC4+ cells, * vs. other groups with different symbols (*, †, ‡, §), P<0.001. F-I. The IF microscopic finding (400×) for identification of TRPC6+ cells (yellow arrows) in PA. J. Number of TRPC6+ cells, * vs. other groups with different symbols (*, †), P<0.001. The scale bars in right lower corner represent 20 μm. All statistical analyses were performed by one-way ANOVA, followed by Bonferroni multiple comparison post hoc test. Symbols (*, †, ‡, §) indicate significance (at 0.05 level). SC = sham control; MCT = monocrotaline; L-mito = low dose of mitochondria; H-mito = high dose of mitochondria.

The immunohistochemical (IHC) microscopic finding of fibrotic area in lung parenchyma displayed an identical pattern of crowded score among the four groups (**Figure 5**). Additionally, the IF microscopic finding showed that the number of TRPC1+ cells in smooth muscle of pulmonary artery (PA), an indicator of smooth muscle proliferation, also displayed an identical pattern of crowded score among four groups (**Figure 5**).

Immunofluorecent (IF) microscopic findings of cellular expressions in PA and lung parenchyma by day 35 after MCT administration

IF microscopic finding showed that the cellular expression of positively-stained TRPC4 in smooth muscle of PA, another indicator of smooth muscle proliferation, was lowest in group 1 and highest in group 2 and significantly higher in group 4 than in group 3 (**Fig-**

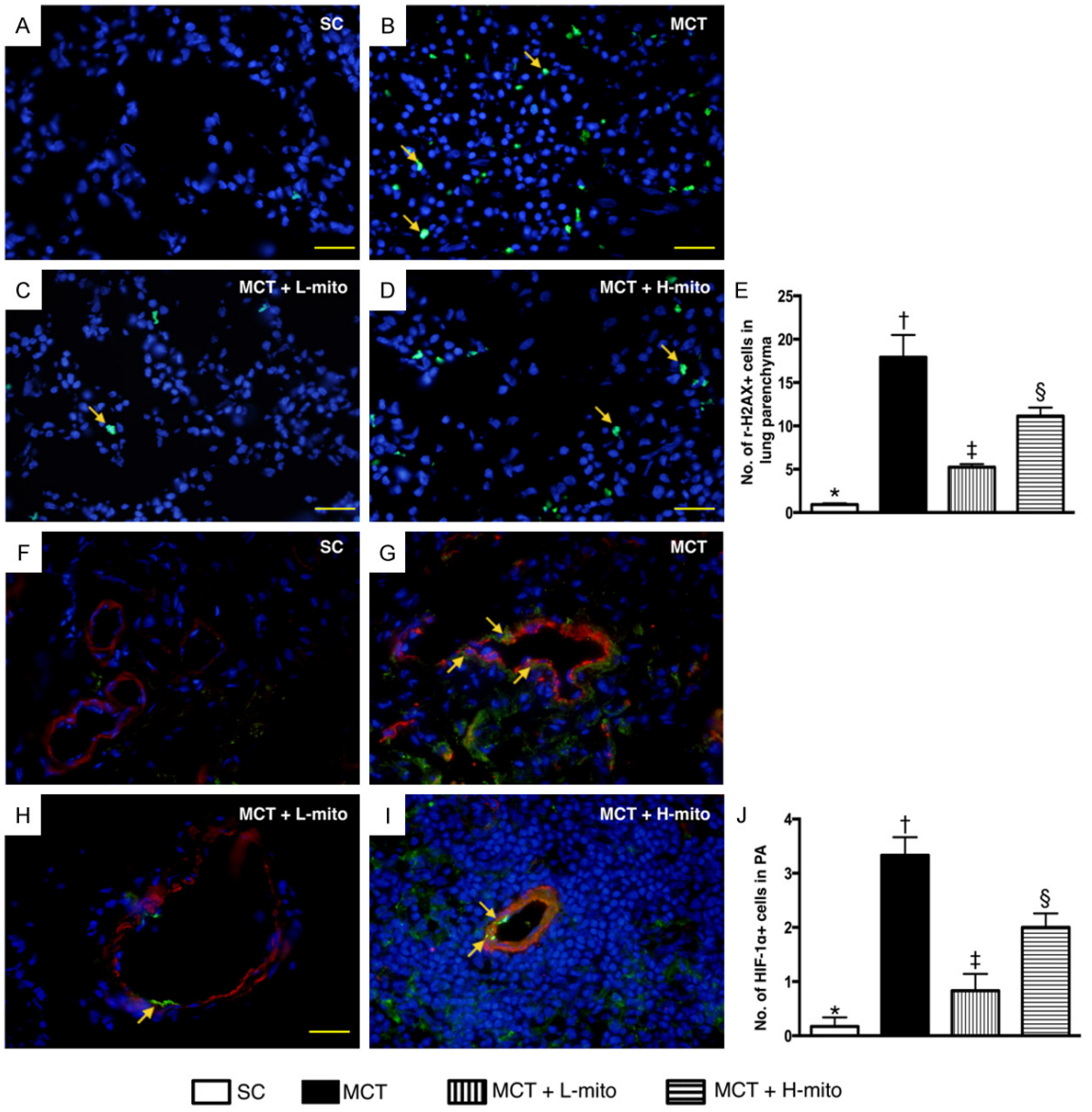

Figure 7. Cellular expressions of DNA-damaged marker in lung parenchyma and hypoxic-inducible marker in pulmonary artery by day 35 after MCT administration. A-D. Immunofluorescent (IF) microscopic finding (400×) for identification of γ-H2AX+ cells (yellow arrows) in lung parenchyma. E. Number of γ-H2AX+ cells, * vs. other groups with different symbols (*, †, ‡, §), P<0.001. F-I. The IF microscopic finding (400×) for identification of hypoxia-inducible factor (HIF)-1α+ cells (yellow arrows) in pulmonary artery (PA). J. Number of HIF-1α+ cells, * vs. other groups with different symbols (*, †), P<0.001. The scale bars in right lower corner represent 20 μm. All statistical analyses were performed by one-way ANOVA, followed by Bonferroni multiple comparison post hoc test. Symbols (*, †, ‡, §) indicate significance (at 0.05 level). SC = sham control; MCT = monocrotaline; L-mito = low dose of mitochondria; H-mito = high dose of mitochondria.

ure 6). Similarly, the cellular expression of positively-stained TRPC6 in smooth muscle of PA was significantly higher in group 2 than in other groups, but it showed no difference among the four groups (**Figure 6**). Additionally, the cellular expressions of positively-stained γ-H2AX in lung parenchyma, an indicator of DNA-damaged marker, showed an identical pattern of TRPC4 among the four groups (**Figure 7**). Furthermore, IF microscopic finding showed that the cellular expression of positively-stained HIF-1α in smooth muscle of PA, an indicator of cells, tissue and organ in response to hypoxic stimulation, displayed an identical pattern of TRPC4 among the four groups (**Figure 7**).

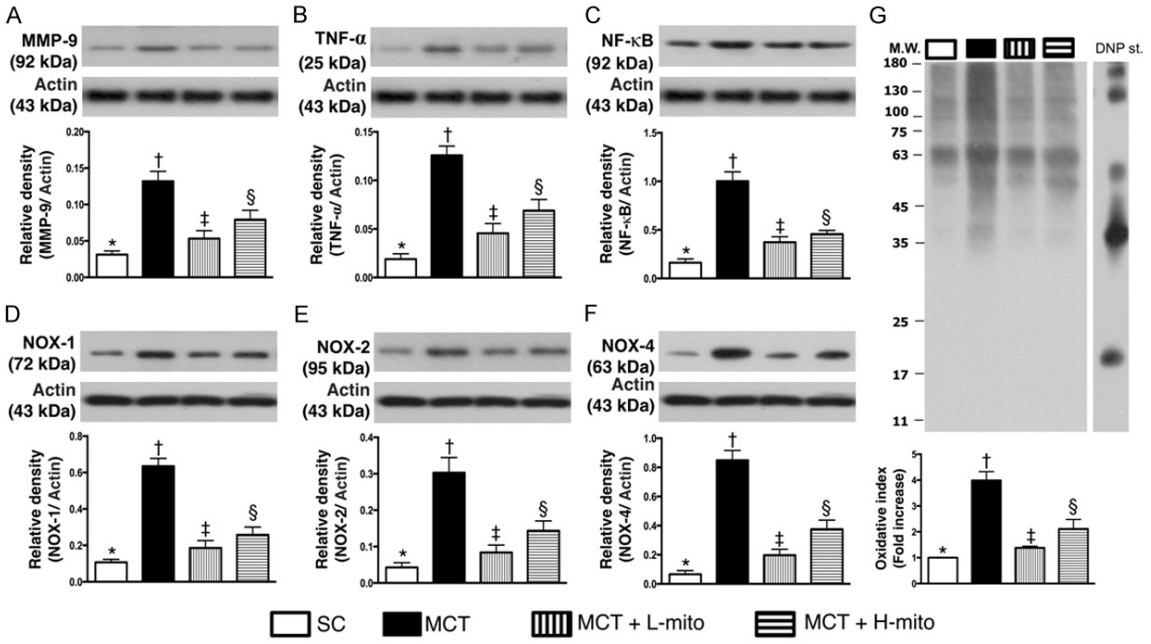

Figure 8. Protein expressions of inflammatory and oxidative stress biomarkers in lung parenchyma by day 35 after MCT administration. A. Protein expression of matrix metalloproteinase (MMP)-9, * vs. other groups with different symbols (*, †, ‡, §), P<0.001. B. Protein expression of tumor necrosis factor (TNF)-α, * vs. other groups with different symbols (*, †, ‡, §), P<0.001. C. Protein expression of nuclear factor (NF)- κB, * vs. other groups with different symbols (*, †, ‡, §), P<0.001. D. Protein expression of NOX-1, * vs. other groups with different symbols (*, †, ‡, §), P<0.001. E. Protein expression of NOX-2, * vs. other groups with different symbols (*, †, ‡, §), P<0.001. F. Protein expression of NOX-4, * vs. other groups with different symbols (*, †, ‡, §), P<0.001. G. Oxidized protein expression, * vs. other groups with different symbols (*, †, ‡, §), P<0.001. (Note: left and tight lanes shown on the upper panel represent protein molecular weight marker and control oxidized molecular protein standard, respectively). M.W = molecular weight; DNP = 1-3 dinitrophenylhydrazone. All statistical analyses were performed by one-way ANOVA, followed by Bonferroni multiple comparison post hoc test. Symbols (*, †, ‡, §) indicate significance (at 0.05 level). SC = sham control; MCT = monocrotaline; L-mito = low dose of mitochondria; H-mito = high dose of mitochondria.

Protein expressions of inflammatory and oxidative stress biomarkers in lung parenchyma by day 35 after MCT administration

The protein expressions of MMP-9, TNF-α, and NF-κB, three indicators of inflammation were highest in group 2 and lowest in group 1, significantly higher in group 4 than in group 3. Additionally, the protein expressions of NOX-1, NOX-2 and NOX-4, three indices of reactive oxygen species (ROS), exhibited an identical pattern of inflammation among the four groups. Furthermore, oxidized protein expression, an indicator of oxidative stress, exhibited an identical pattern of ROS among the four groups (**Figure 8**).

Protein expressions of apoptotic, fibrotic and anti-fibrotic markers in lung parenchyma by day 35 after MCT administration

The protein expressions of Bax and cleaved caspase 3 and PRAP, three indicators of apoptosis, were significantly higher in group 2 than in other groups, significantly higher in group 4 than in groups 1 and 3, and significantly higher in group 3 than in group 1. Additionally, the protein expressions of Smad3 and TGF-β, two indicators of fibrosis, showed an identical pattern of apoptosis. Conversely, phosphorylated (p)-Smad1, p-Sam5 and BMP-2, three indicators of anti-apoptosis, displayed an opposite pattern of inflammation among the four groups (**Figure 9**).

Protein expressions of pressure-overload and hypoxia-induced smooth contraction and proliferation biomarkers in lung parenchyma by day 35 after MCT administration

The protein expressions of TRPC1 (**Figure 10A**), TRPC4 (**Figure 10B**) and TRPC6 (**Figure 10C**), three indices in regulating smooth muscle cell contraction and proliferation, were significantly higher in group 2 than in other groups, significantly higher in group 4 than in groups 1 and 3,

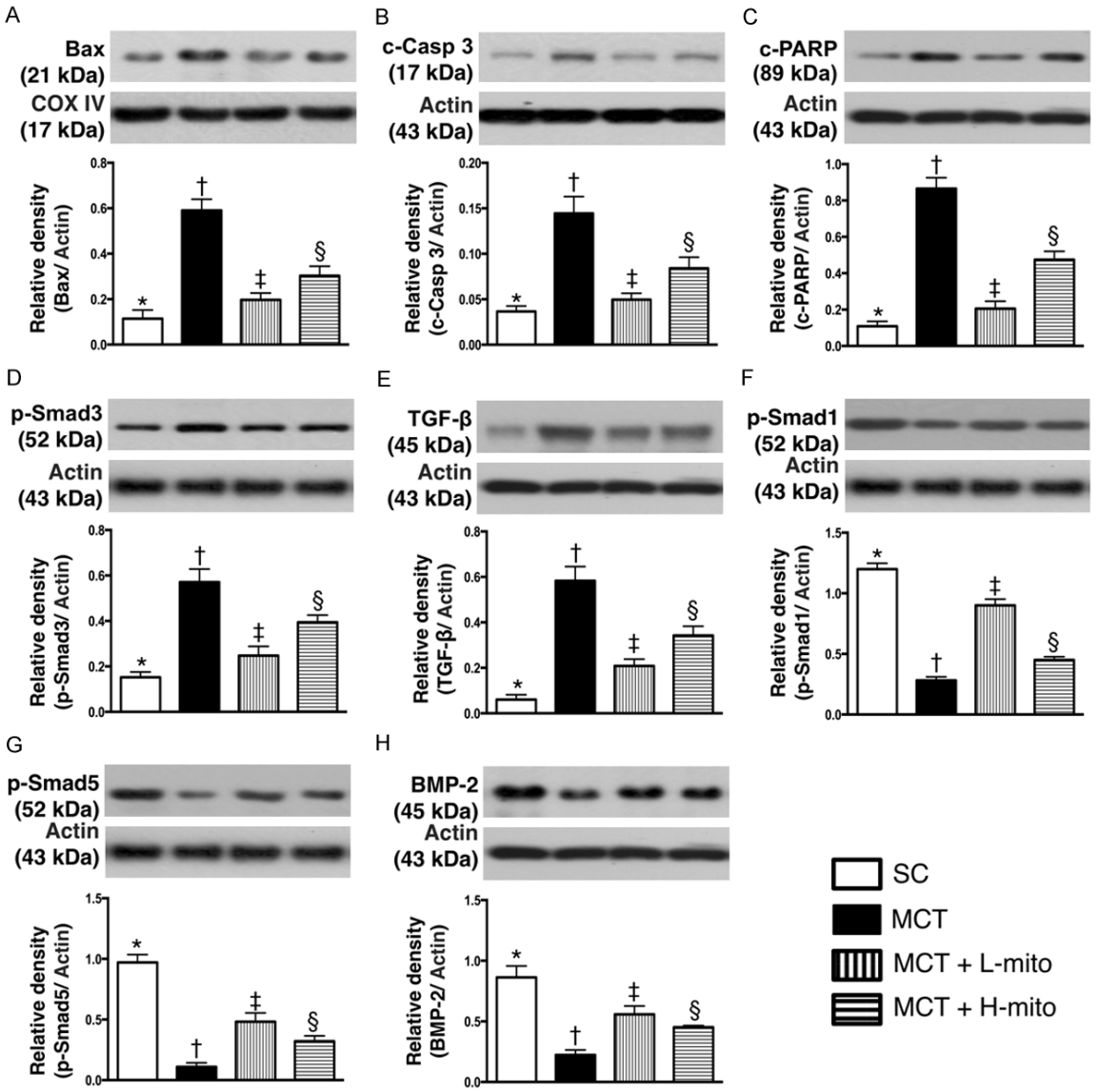

Figure 9. Protein expressions of apoptotic, fibrotic and anti-fibrotic markers in lung parenchyma by day 35 after MCT administration. A. Protein expression of Bax, * vs. other groups with different symbols (*, †, ‡, §), P<0.001. B. Protein expression of cleaved caspase 3, * vs. other groups with different symbols (*, †, ‡, §), P<0.001. C. Protein expression of cleaved poly (ADP-ribose) polymerase (c-PARP), * vs. other groups with different symbols (*, †, ‡, §), P<0.001. D. Protein expression of phosphorylated (p)-Smad3, * vs. other groups with different symbols (*, †, ‡, §), P<0.001. E. Protein expression of transforming growth factor (TGF)-β, * vs. other groups with different symbols (*, †, ‡, §), P<0.001. F. Protein expression of p-Smad1, * vs. other groups with different symbols (*, †, ‡, §), P<0.001. G. Protein expression of p-Smad5, * vs. other groups with different symbols (*, †, ‡, §), P<0.001. H. Protein expression of bone morphogenetic protein (BMP)-2, * vs. other groups with different symbols (*, †, ‡, §), P<0.001. All statistical analyses were performed by one-way ANOVA, followed by Bonferroni multiple comparison post hoc test. Symbols (*, †, ‡, §) indicate significance (at 0.05 level). SC = sham control; MCT = monocrotaline; L-mito = low dose of mitochondria; H-mito = high dose of mitochondria.

and significantly higher in group 3 than in group 1. Additionally, protein expressions of HIP-1α (**Figure 10E**), a factor in response to hypoxia stimulation and connexin43 (**Figure 10D**), an indicator of pressure-overload and hypoxia stimulation, showed an identical pattern of TRPCs among the four groups.

Protein expression of mitochondrial damaged biomarker in lung parenchyma by day 35 after MCT administration

The protein expression of cytosolic cytochrome C (**Figure 10E**), and indicator of mitochondrial damage, was highest in group 2 and lowest in

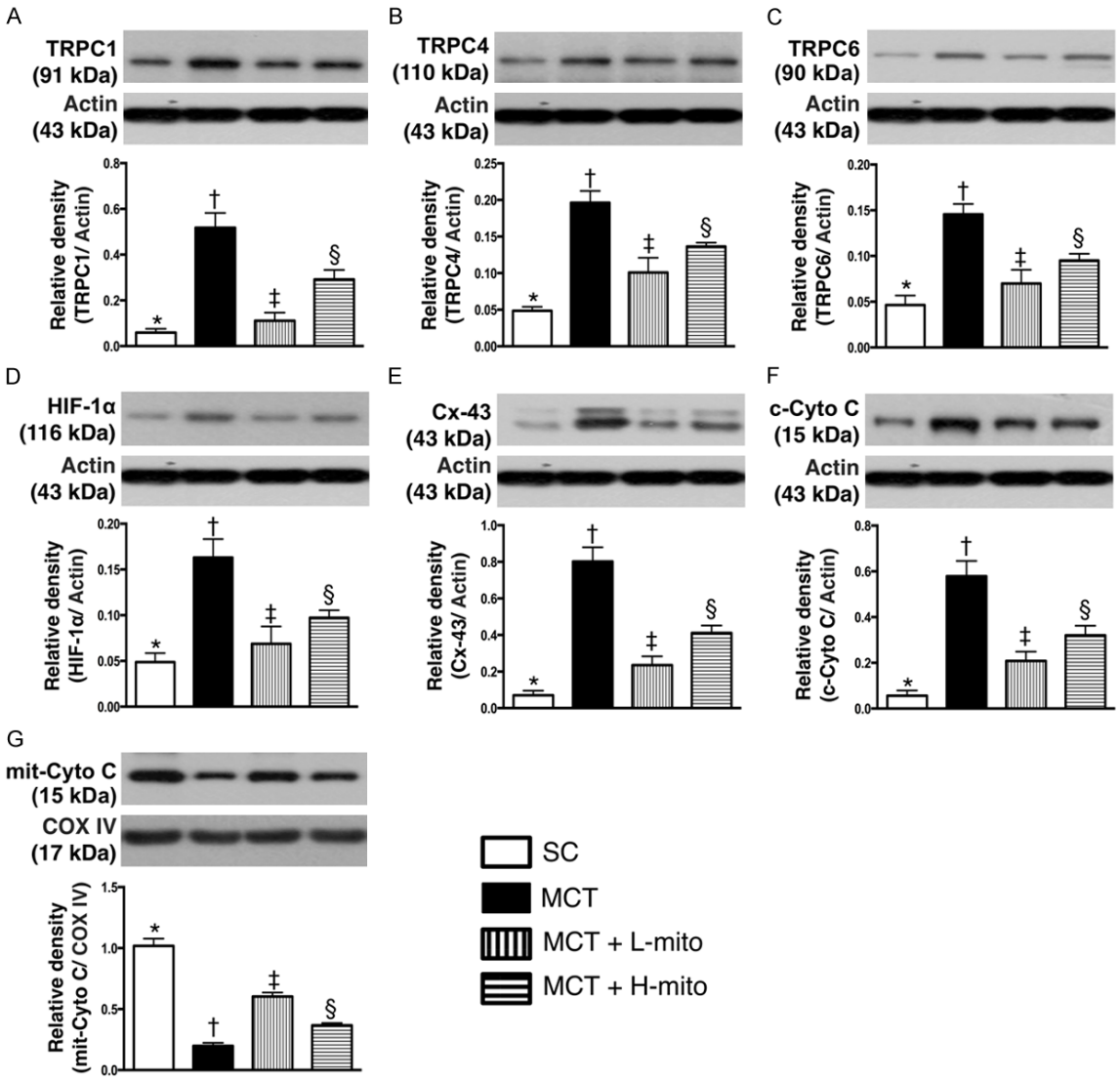

Figure 10. Protein expressions of pressure-overload and hypoxia-induced smooth contraction TRPCs, HIF-1, Cx43 and mitochondrial damaged markers in lung parenchyma by day 35 after MCT administration. A. Protein expression of transient receptor potential cation channel (TRPC) 1, * vs. other groups with different symbols (*, †, ‡, §), P<0.001. B. Protein expression of TRPC4, * vs. other groups with different symbols (*, †, ‡, §), P<0.001. C. Protein expression of TRPC6, * vs. other groups with different symbols (*, †, ‡, §), P<0.001. D. Protein expression of hypoxic inducible factor (HIF)-1α, * vs. other groups with different symbols (*, †, ‡, §), P<0.001. E. Protein expression of connexin(Cx)43, * vs. other groups with different symbols (*, †, ‡, §), P<0.001. F. Protein expression of cytosolic cytochrome C (Cyt-cyto C), * vs. other groups with different symbols (*, †, ‡, §), P<0.001. G. Protein expression of mitochondrial cytochrome C (Mit-cyto C), * vs. other groups with different symbols (*, †, ‡, §), P<0.001. All statistical analyses were performed by one-way ANOVA, followed by Bonferroni multiple comparison post hoc test. Symbols (*, †, ‡, §) indicate significance (at 0.05 level). SC = sham control; MCT = monocrotaline; L-mito = low dose of mitochondria; H-mito = high dose of mitochondria.

group 1, and significantly higher in group 4 than in group 3. On the other hand, the protein expression of mitochondrial cytochrome C (**Figure 10F**), an indicator of mitochondrial preservation, showed an opposite pattern of cytosolic cytochrome C among the four groups (**Figure 10**).

Discussion

This study which investigated the therapeutic impact of mitochondria transfusion on protecting against MCT-induced PAH presented following important findings. First, mitochondria treatment was found to be effective on restora-

tion of pulmonary (i.e., improved saO_2) and circulatory (i.e., reduced RVSBP) functions in the setting of MCT-induced PAH. Second, mitochondria therapy remarkably attenuated MCT-induced lung parenchymal injury (i.e., attenuated lung injury score and preserved number of alveolar sacs) as well as reduced the proliferation of smooth muscle in pulmonary artery (i.e., ameliorated number of muscularized arteries and TRPCs). Third, mitochondria therapy inhibited the cellular-molecular perturbations (i.e., inhibiting the expressions of oxidative stress, apoptosis, inflammation and mitochondrial damage). Finally, the paradoxical effect of low dose of mitochondria was superior to high dose of mitochondria for protecting against MCT-induced PAH, indicating that a over dose of mitochondria has been utilized in the present study.

The lungs maintain their unique function in gaseous exchange through their remarkably large alveolar surface area, their rich and delicate alveolar capillary network, as well as their normal physical properties (i.e., elasticity and compliance) [20]. Thus, to identification of the lung disease entity is not only from histopathological findings but also from deterioration of its functional capacity. Two essential findings in the present study were that the RVSBP (i.e., an indirect reflector of pulmonary blood pressure) was remarkably higher, whereas the saO_2 (i.e., lung function capacity) was notably lower in MCT-treated animals as compared to those of SC animals. These two abnormal circulatory and functional indices of lung that were found in the present study were consistent with the findings of our previous studies in setting of MCT-induced PAH [10-12, 19]. The most important finding in the present study was that both the RVSBP and saO_2 were substantially revised in those of MCT-treated animals after receiving early (i.e., at day 5 after MCT administration) mitochondrial transfusion therapy. Intriguingly, we have recently demonstrated that systemic administration of mitochondria improved saO_2 and normalized the RVSBP in rat after acute respiratory distress syndrome (ARDS) [20]. Therefore, our present and recent reported [20] studies, in addition to supporting each other, highlight the beneficial effect of mitochondria therapy on setting of acute lung injury. In fact, some data have recently shown the protective effect of mitochondria therapy on acute organ injury [16-18]. Accordingly, the results of our present study corroborated with the findings from those of recent studies [16-18, 20].

When we looked at the results of histopathological findings of the lung parenchyma, we found that the lung crowded score, the expressions of TRPCs in pulmonary arteries, number of muscularized arteries (i.e., pulmonary arterial remodeling) and fibrotic area were significantly increased, whereas the numbers of alveolar sacs and small vessels were notably reduced in MCT-treated animals than in SC animals. These histopathological findings were very common to be identified in animals model of MCT-induced [10-12, 19] or hypoxia-induced [24] PAH. The principal finding in the present study was that these abnormal histopathological findings were significantly reversed in MCT-treated animals after receiving mitochondria treatment. Interestingly, our recent study also showed that mitochondria therapy significantly conversed these histopathological expressions in lung parenchyma of ARDS animals [20]. In this way, the results of the present study not only reinforced the findings of our recent study [20] but also could explain why the RVSBP was remarkably attenuated, whereas the saO_2 was markedly improved in MCT-treated animals after receiving mitochondria transfusion.

The crucial role of ROS and oxidative stress on endothelial dysfunction, tissue damage, cellular apoptosis and development of hypertension has been well recognized in the past several decades. Another essential finding in the present study was that the generations of ROS (i.e., NOX-1, NOX-2, NOX4) and oxidative stress (i.e., oxidized protein) were substantially augmented in MCT-treated animals as compared with those of SC animals. Of particular importance was that the productions of ORS and oxidative stress were significantly attenuated in MCT-treated animals after receiving mitochondria therapy. Interestingly, in an ARDS animal model, our recent study has also identified that mitochondria therapy notably reduced the generations of ROS and oxidative stress. Accordingly, these two studies were consistent and support that mitochondria therapy offers benefit on protecting lung against damage from MCT-induced PAH and ARDS that may be mainly through ameliorating the generations of ROS and oxidative stress.

Enhancement of inflammation, apoptosis and fibrosis have been identified as three key biomarkers involved in experimental model of MCT-induced PAH [10-12, 19]. The results of the present study revealed that the protein expressions of the inflammatory, apoptotic and fibrotic biomarkers as well as the cellular expression of DNA-damaged marker were remarkably enhanced, whereas the anti-fibrotic biomarkers were substantially suppressed in MCT-treated animals as compared to those of SC animals. Additionally, the protein expression of connexin43, an index of regulating smooth muscle proliferation in response to hypoxia and pressure overload in early stage of MCT-induced PAH, was markedly augmented in MCT-treated animals than in SC animals. Our findings were comparable with the findings of previous studies [10-12, 19]. Of particular importance was that these parameters were notably reversed after mitochondria treatment.

We remain uncertain for what is the exactly underlying mechanism involving in mitochondria transfusion improved MCT-induced PAH. Perhaps it could be mainly due to the replacement of exogenous mitochondria into the cells which were just ongoing the process of endogenous mitochondria damage with production of oxidative stress and exhausting energy. This mitochondrial refreshing process could extinguish the further production of ROS and oxidative stress in the injured cells. Our distinctive findings of cytosolic cytochrome C was markedly reduced, whereas the mitochondrial cytochrome C was markedly increased could, at least in part, support our hypothesis.

Disclosure of conflict of interest

None.

Address correspondence to: Dr. Hon-Kan Yip, Division of Cardiology, Department of Internal Medicine, Kaohsiung Chang Gung Memorial Hospital and Chang Gung University College of Medicine, Taiwan123, Dapi Road, Niaosung District, Kaohsiung 83301, Taiwan. Tel: +886-7-7317123; Fax: +886-7-7322402; E-mail: han.gung@msa.hinet.net

References

[1] Hoeper MM, Bogaard HJ, Condliffe R, Frantz R, Khanna D, Kurzyna M, Langleben D, Manes A, Satoh T, Torres F, Wilkins MR and Badesch DB. Definitions and diagnosis of pulmonary hypertension. J Am Coll Cardiol 2013; 62: D42-50.

[2] D'Alonzo GE, Barst RJ, Ayres SM, Bergofsky EH, Brundage BH, Detre KM, Fishman AP, Goldring RM, Groves BM, Kernis JT and et al. Survival in patients with primary pulmonary hypertension. Results from a national prospective registry. Ann Intern Med 1991; 115: 343-349.

[3] Gaine SP and Rubin LJ. Primary pulmonary hypertension. Lancet 1998; 352: 719-725.

[4] Pietra GG, Edwards WD, Kay JM, Rich S, Kernis J, Schloo B, Ayres SM, Bergofsky EH, Brundage BH, Detre KM and et al. Histopathology of primary pulmonary hypertension. A qualitative and quantitative study of pulmonary blood vessels from 58 patients in the National Heart, Lung, and Blood Institute, Primary Pulmonary Hypertension Registry. Circulation 1989; 80: 1198-1206.

[5] Rubin LJ. Primary pulmonary hypertension. N Engl J Med 1997; 336: 111-117.

[6] Rubin LJ and Badesch DB. Evaluation and management of the patient with pulmonary arterial hypertension. Ann Intern Med 2005; 143: 282-292.

[7] Runo JR and Loyd JE. Primary pulmonary hypertension. Lancet 2003; 361: 1533-1544.

[8] Ryan JJ, Huston J, Kutty S, Hatton ND, Bowman L, Tian L, Herr JE, Johri AM and Archer SL. Right ventricular adaptation and failure in pulmonary arterial hypertension. Can J Cardiol 2015; 31: 391-406.

[9] Eddahibi S, Guignabert C, Barlier-Mur AM, Dewachter L, Fadel E, Dartevelle P, Humbert M, Simonneau G, Hanoun N, Saurini F, Hamon M and Adnot S. Cross talk between endothelial and smooth muscle cells in pulmonary hypertension: critical role for serotonin-induced smooth muscle hyperplasia. Circulation 2006; 113: 1857-1864.

[10] Sun CK, Lee FY, Sheu JJ, Yuen CM, Chua S, Chung SY, Chai HT, Chen YT, Kao YH, Chang LT and Yip HK. Early combined treatment with cilostazol and bone marrow-derived endothelial progenitor cells markedly attenuates pulmonary arterial hypertension in rats. J Pharmacol Exp Ther 2009; 330: 718-726.

[11] Sun CK, Lin YC, Yuen CM, Chua S, Chang LT, Sheu JJ, Lee FY, Fu M, Leu S and Yip HK. Enhanced protection against pulmonary hypertension with sildenafil and endothelial progenitor cell in rats. Int J Cardiol 2012; 162: 45-58.

[12] Yen CH, Tsai TH, Leu S, Chen YL, Chang LT, Chai HT, Chung SY, Chua S, Tsai CY, Chang HW, Ko SF, Sun CK and Yip HK. Sildenafil improves long-term effect of endothelial progenitor cell-based treatment for monocrotaline-induced rat pulmonary arterial hypertension. Cytotherapy 2013; 15: 209-223.

[13] Crosswhite P and Sun Z. Nitric oxide, oxidative stress and inflammation in pulmonary arterial hypertension. J Hypertens 2010; 28: 201-212.
[14] Rungatscher A, Hallstrom S, Linardi D, Milani E, Gasser H, Podesser BK, Scarabelli TM, Luciani GB and Faggian G. S-nitroso human serum albumin attenuates pulmonary hypertension, improves right ventricular-arterial coupling, and reduces oxidative stress in a chronic right ventricle volume overload model. J Heart Lung Transplant 2015; 34: 479-488.
[15] Doughan AK, Harrison DG and Dikalov SI. Molecular mechanisms of angiotensin II-mediated mitochondrial dysfunction: linking mitochondrial oxidative damage and vascular endothelial dysfunction. Circ Res 2008; 102: 488-496.
[16] Islam MN, Das SR, Emin MT, Wei M, Sun L, Westphalen K, Rowlands DJ, Quadri SK, Bhattacharya S and Bhattacharya J. Mitochondrial transfer from bone-marrow-derived stromal cells to pulmonary alveoli protects against acute lung injury. Nat Med 2012; 18: 759-765.
[17] Masuzawa A, Black KM, Pacak CA, Ericsson M, Barnett RJ, Drumm C, Seth P, Bloch DB, Levitsky S, Cowan DB and McCully JD. Transplantation of autologously derived mitochondria protects the heart from ischemia-reperfusion injury. Am J Physiol Heart Circ Physiol 2013; 304: H966-982.
[18] Lin HC, Liu SY, Lai HS and Lai IR. Isolated mitochondria infusion mitigates ischemia-reperfusion injury of the liver in rats. Shock 2013; 39: 304-310.
[19] Yen CH, Leu S, Lin YC, Kao YH, Chang LT, Chua S, Fu M, Wu CJ, Sun CK and Yip HK. Sildenafil limits monocrotaline-induced pulmonary hypertension in rats through suppression of pulmonary vascular remodeling. J Cardiovasc Pharmacol 2010; 55: 574-584.
[20] Sun CK, Lee FY, Kao YH, Chiang HJ, Sung PH, Tsai TH, Lin YC, Leu S, Wu YC, Lu HI, Chen YL, Chung SY, Su HL and Yip HK. Systemic combined melatonin-mitochondria treatment improves acute respiratory distress syndrome in the rat. J Pineal Res 2015; 58: 137-150.
[21] Yip HK, Chang YC, Wallace CG, Chang LT, Tsai TH, Chen YL, Chang HW, Leu S, Zhen YY, Tsai CY, Yeh KH, Sun CK and Yen CH. Melatonin treatment improves adipose-derived mesenchymal stem cell therapy for acute lung ischemia-reperfusion injury. J Pineal Res 2013; 54: 207-221.
[22] Chen YT, Chiang HJ, Chen CH, Sung PH, Lee FY, Tsai TH, Chang CL, Chen HH, Sun CK, Leu S, Chang HW, Yang CC and Yip HK. Melatonin treatment further improves adipose-derived mesenchymal stem cell therapy for acute interstitial cystitis in rat. J Pineal Res 2014; 57: 248-261.
[23] Chen HH, Chang CL, Lin KC, Sung PH, Chai HT, Zhen YY, Chen YC, Wu YC, Leu S, Tsai TH, Chen CH, Chang HW and Yip HK. Melatonin augments apoptotic adipose-derived mesenchymal stem cell treatment against sepsis-induced acute lung injury. Am J Transl Res 2014; 6: 439-458.
[24] Sun CK, Zhen YY, Lu HI, Sung PH, Chang LT, Tsai TH, Sheu JJ, Chen YL, Chua S, Chang HW, Chen YL, Lee FY and Yip HK. Reducing TRPC1 Expression through Liposome-Mediated siRNA Delivery Markedly Attenuates Hypoxia-Induced Pulmonary Arterial Hypertension in a Murine Model. Stem Cells Int 2014; 2014: 316214.